Optical Simulation

Howard Wang

Experiment Briefs

- Lens: Throlabs LB1761 BK7 biconvex lens (f/8 aperture, 2 mm from the 2nd surface)
- Parameters: R1 = 24.5, T = 9, R2 = -24.5, D2 = 22.2, OD = 3.175 mm
- Experiments:
  - Function test
  - Layout & Ray visualization
  - Focus estimation
  - N, λ, D2, OD sweep
  - Off-axis sweep

Lens Visualization

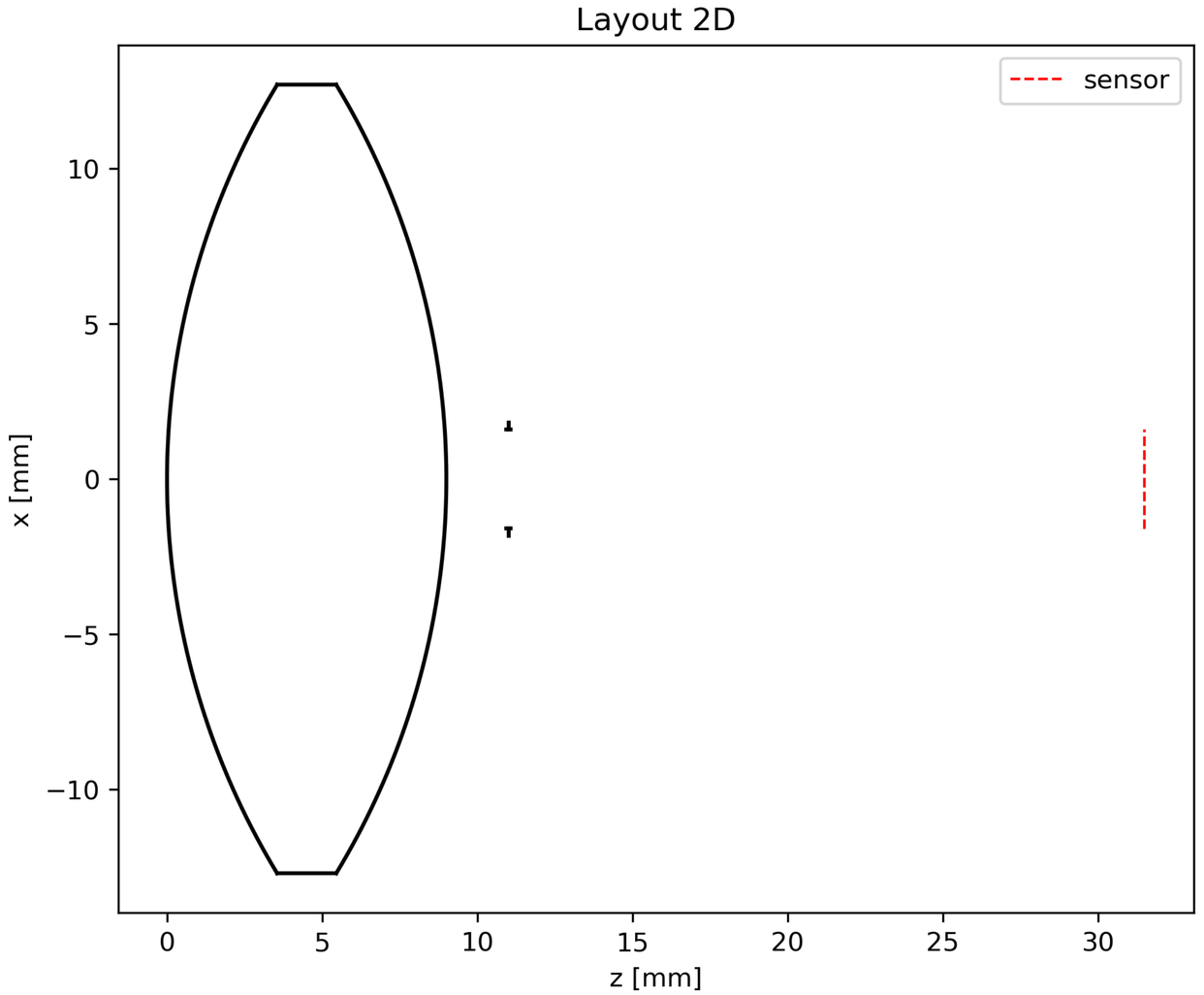

PSF Examples

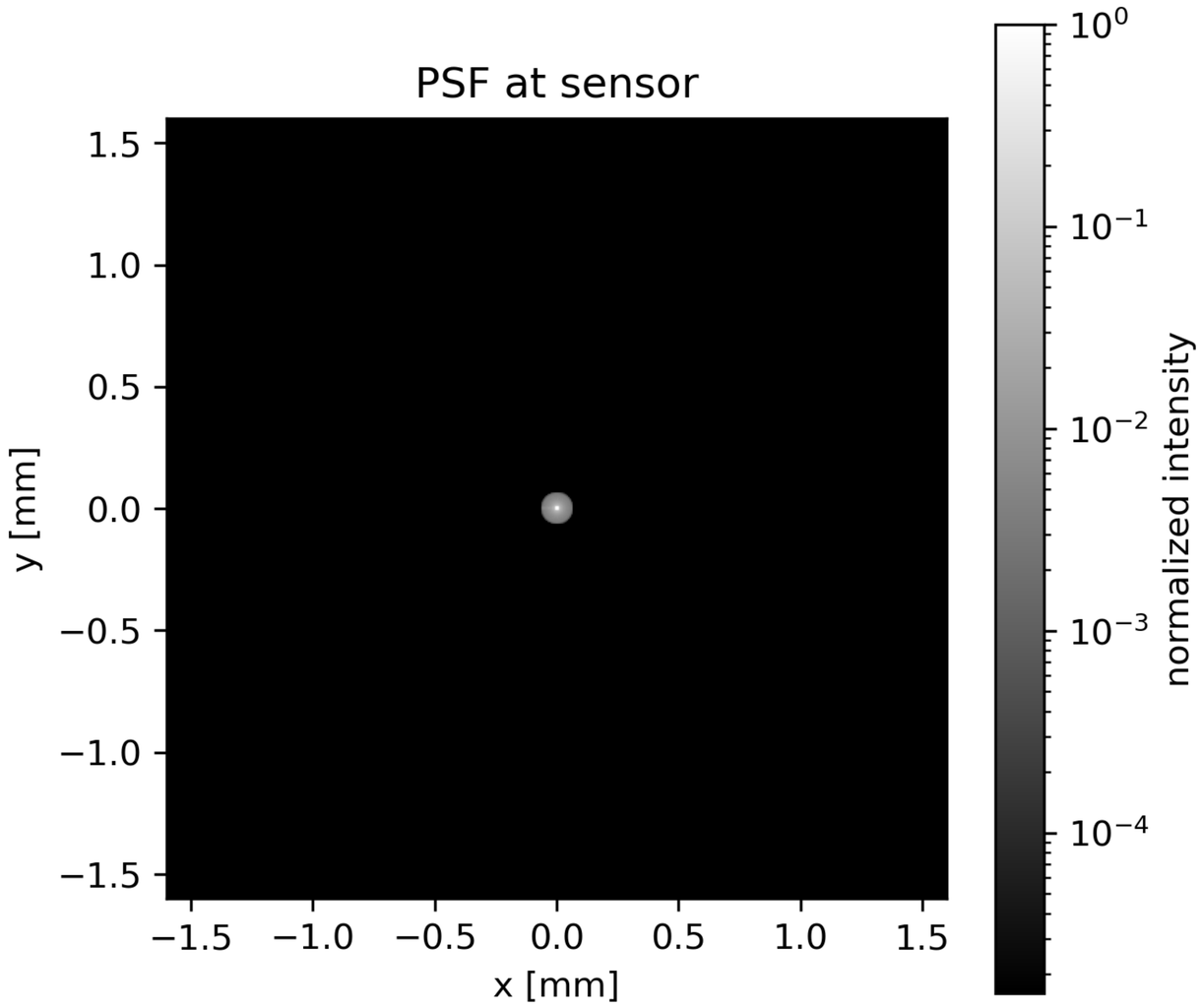

R1 = 24.5, T = 9, R2 = -24.5, D2 = 22.2, OD = 6.35 mm, N = 3200

Best focus

Aperture (mm)	1.6 (f/16)	3.175 (f/8)	6.35 (f4)	12.7 (f/2)
Best focus distance	20.55	20.5	20.3	18.7

The best sensor-to-aperture distance varies slightly with aperture size, showing a shift from 20.55 mm at f/16 to 18.7 mm at f/2 due to increased spherical aberration at larger apertures.

Sampling N Sweep

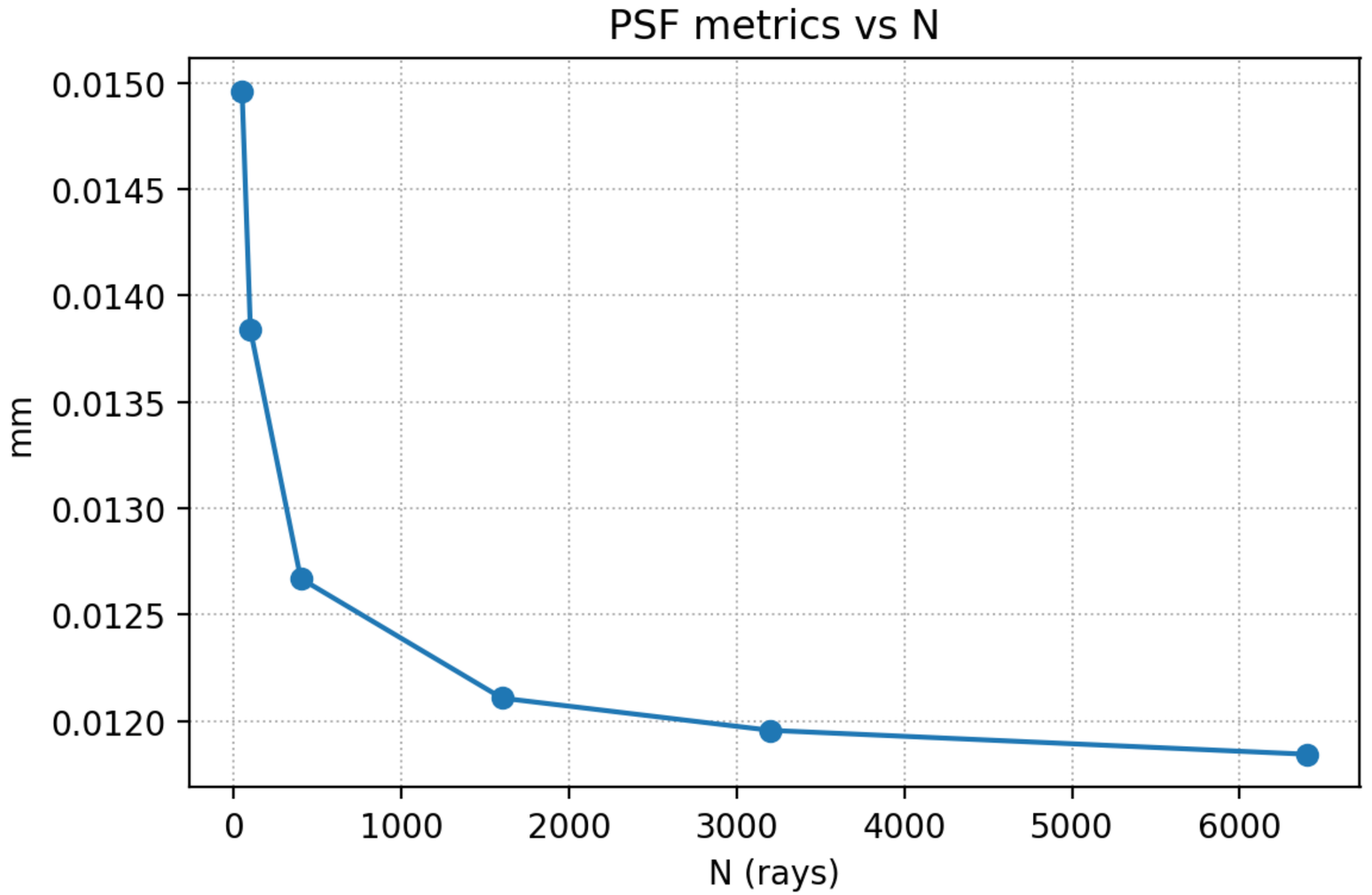

The convergence begins around N ≥ 1600, where the RMS values stabilize to ~0.045 mm and ~0.021 mm, respectively — indicating sufficient ray sampling density for accurate PSF estimation. To get better simulation, we choose N=3200 for the rest of experiments.

Wavelength λ Sweep

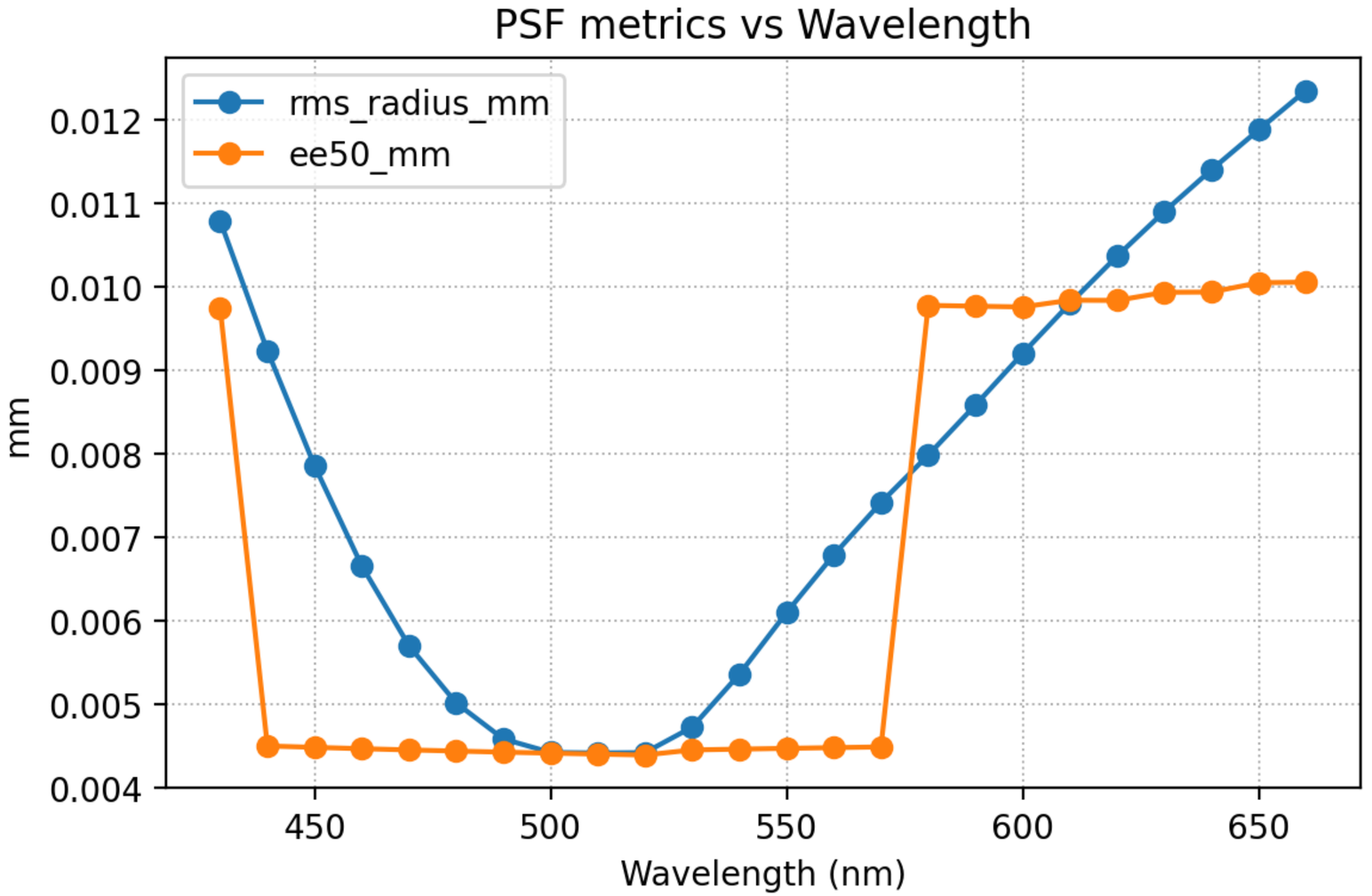

With BK7 dispersion enabled, the smallest PSF occurs near ~500 nm and grows toward both spectral ends. This matches expectation: the effective focal length shifts with λ (chromatic focus), so a single sensor position cannot be perfectly focused for all wavelengths. (EE 50 has limitation here)

Focus D2 Sweep

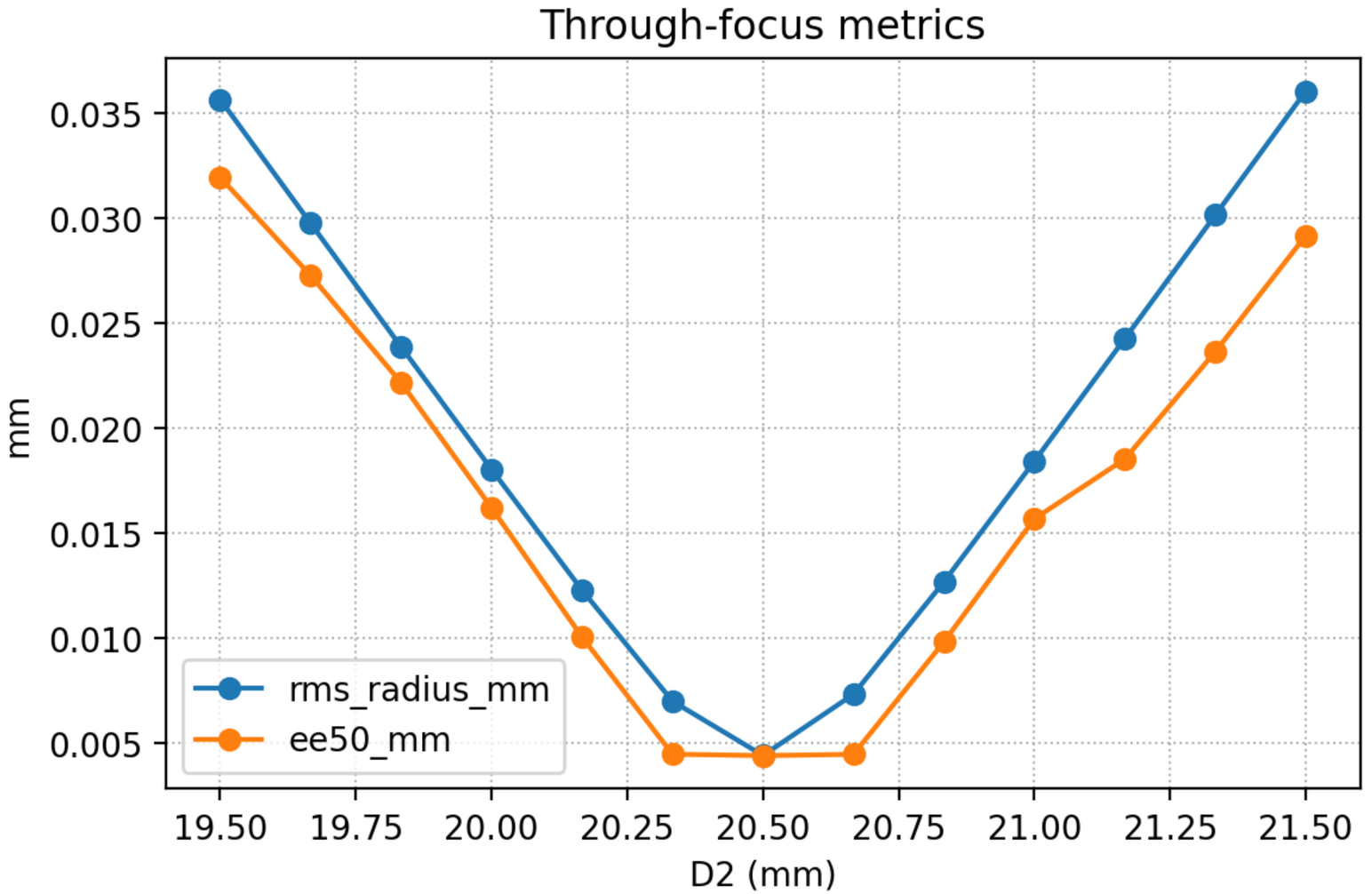

As we move away from 20.5 mm (toward 20.33 or 20.66 and beyond), RMS and EE50 grow smoothly, indicating increasing defocus blur. The growth is slightly asymmetric—typical once real lens aberrations are present. The sweep cleanly identifies 20.5 mm as the optimal aperture-to-sensor distance for this configuration, with predictable defocus behavior on either side.

Aperture OD Sweep

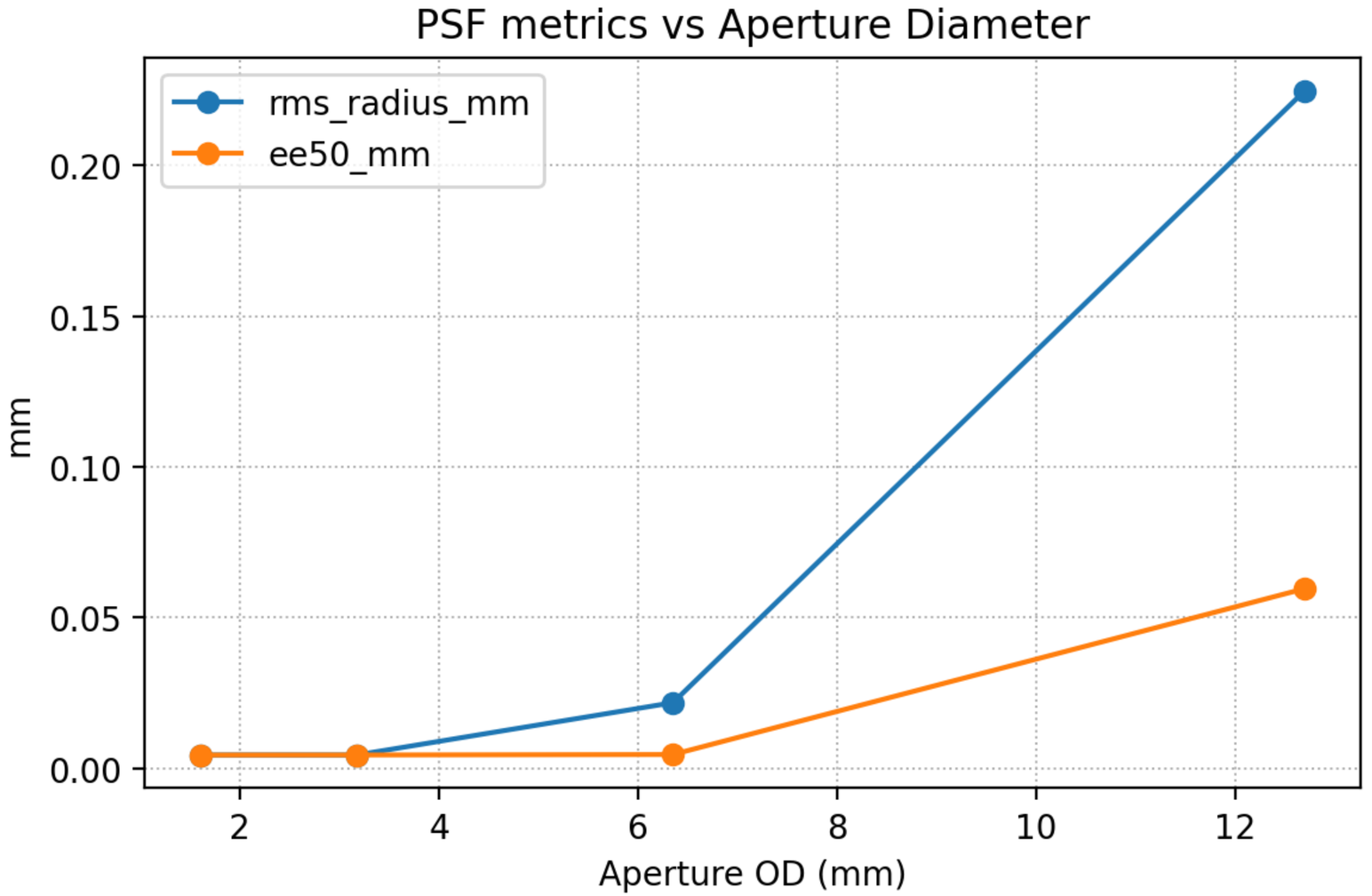

As aperture increases from ~1.6→12.7 mm, the PSF's core (EE50) stays nearly constant at small–moderate apertures while the halo (RMS) grows rapidly—and at the largest aperture both EE50 and RMS spike—so the sharpest results occur with small apertures (~1.6–3.2 mm).

Off-axis sweep

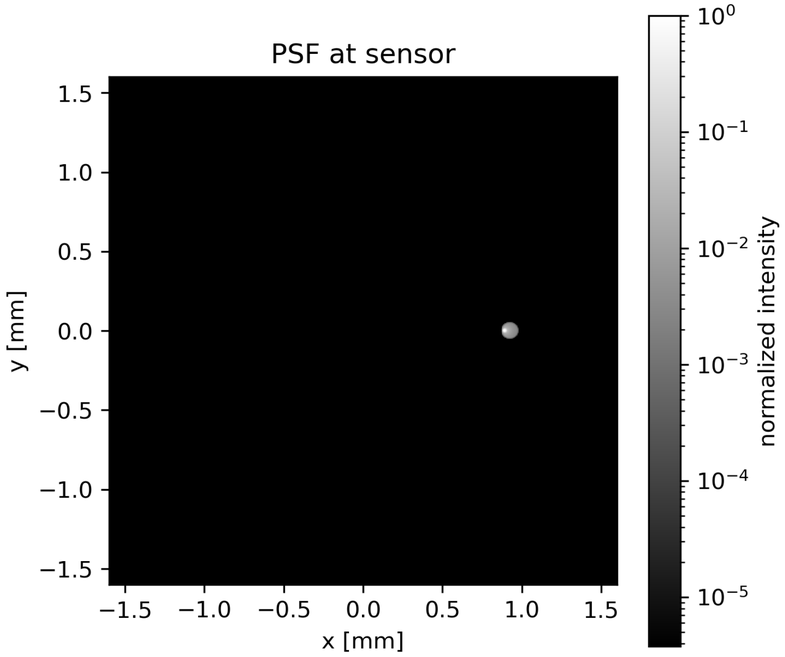

$X_{off} = -35mm$

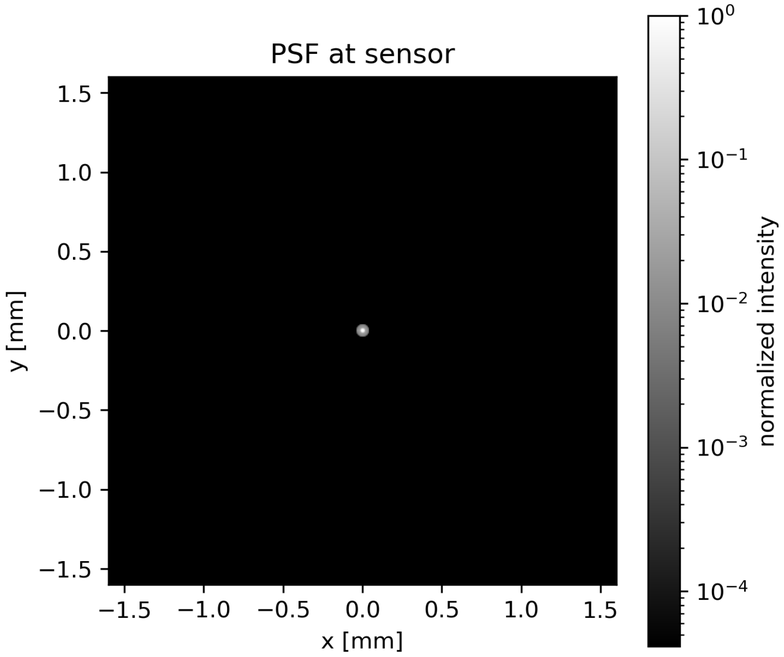

$X_{off} = 0mm$

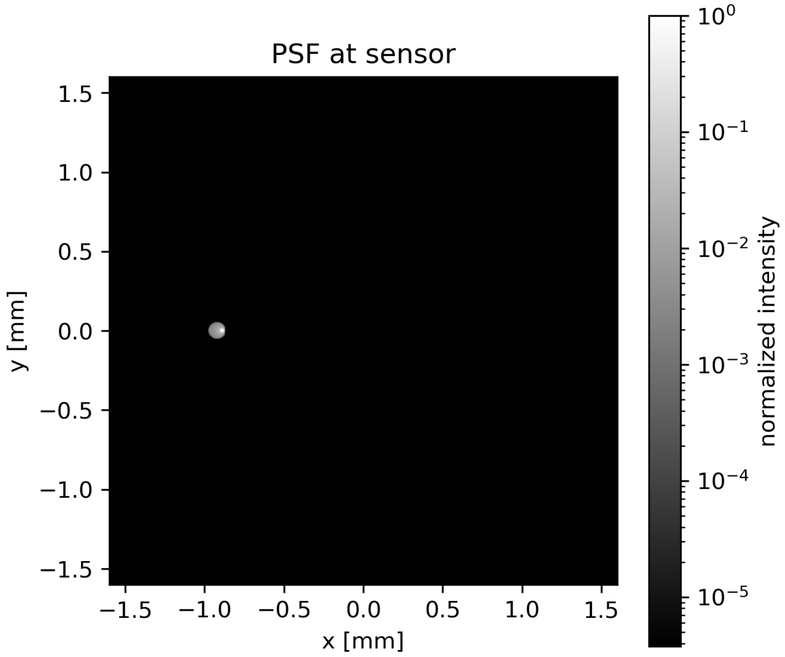

$X_{off} = 35mm$

Off-axis sweep

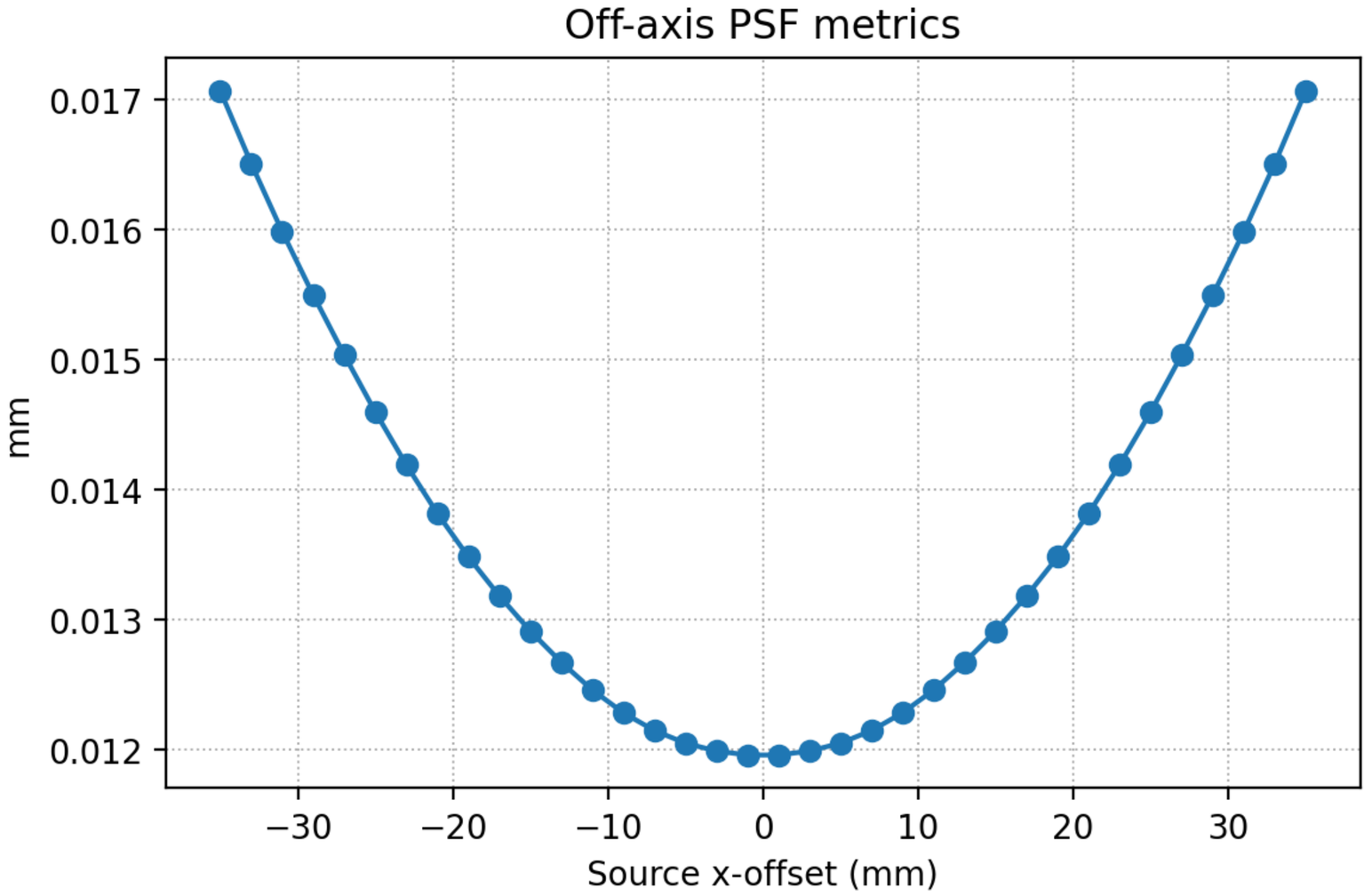

As the source moves off-axis, the PSF centroid shifts roughly linearly with field while the core size stays nearly constant for small offsets, with only mild broadening/asymmetry (coma) appearing as the field angle increases.

Qualitative Analysis

- Sampling: convergence at $N \geq 1600$, aliasing at low N
- Wavelength: chromatic aberration
- Focus: symmetric degradation around best focus (20.5 mm)
- Aperture: sharpness
- Off-axis: coma

Aberration Correction Comparison

Aspect	Classical Deconvolution	Neural Network Approach
Principle	Linear inversion (e.g., Wiener, RL) using known PSF	Data-driven mapping from blurred to sharp
Pros	Physically interpretable; predictable behavior; easy to regularize; no training data	Can handle complex, non-paraxial, chromatic, or field-dependent aberrations; flexible and adaptive.
Cons	Sensitive to noise and PSF mismatch; performance drops when aberrations vary across field.	Requires training data, risk of overfitting
Best use	Mild blur, stationary PSF	Complex senarios, data-rich pipelines.

Comparison classical deconvolution method and neural network approach

Model Refinement

- Physical accuracy:
  - Add diffraction, pixel MTF, temperature tolerances
- Computational efficiency:
  - Vectorization of intersection, GPU acceleration
- Extensions:
  - Image rendering, multi-lens systems